

Structure and Dynamics of Adenosine Triphosphate–Al(III) Complexes at pH 7.4

Ivo Dellavia, Johan Blixt, Claude Dupressoir, and Christian Detellier*

Ottawa-Carleton Chemistry Institute, Department of Chemistry, University of Ottawa, Ottawa, Ontario K1N 6N5, Canada

Received November 10, 1993*

The interaction of Al(III) with adenosine 5'-triphosphate (ATP) was investigated at pH = 7.4 by ^{31}P , ^{13}C , ^1H , and ^{27}Al NMR. Two complexes coexist in equilibrium: 2:1 and a 1:1 complexes, $\text{Al}^{\text{III}}(\text{ATP})_2$ and $\text{Al}^{\text{III}}(\text{ATP})$. Their phenomenological equilibrium constants of formation were calculated from the ^{31}P NMR data. They are in good agreement with independently determined thermodynamic equilibrium constants (Kiss, T.; Sovago, I.; Martin, R. B. *Inorg. Chem.* 1991, 30, 2130–2132). The exchange rate between free and Al(III)-bound ATP (in the 2:1 complex) was determined from a ^{31}P - ^{31}P EXSY experiment to be 3.4 s^{-1} at 295 K, a value diagnostic of a dissociative mechanism from octahedral Al(III). The rate of exchange is probably governed by the rupture of the Al(III)-phosphate bonds, the Al(III)-ATP 1:1 complex being an intermediate in the exchange process. The ^{31}P NMR resonances of the complexes are broad. In the case of the 2:1 complex, since the line widths are linearly related to the square of the field of observation, while the longitudinal relaxation rates are independent of this field, the broadening could be ascribed to relatively fast exchange of two or more forms of this 2:1 complex. At 270 K, at least four signals could be observed for the complexed β - ^{31}P . The possible attribution of these signals to various diastereoisomers of the 2:1 complex is discussed.

Introduction

Even if aluminum is the most abundant metal and represents 8.1% of total earth crust, it is only recently that a strong interest has aroused about its biological roles.¹ Aluminum has often been found associated with amyloid proteins forming neurofibrillary tangles in case of Alzheimer's disease,^{1c} and there is an animated controversy in the literature on its measurement in brain tissues.² A recent geographical study has established a positive correlation between Al in drinking water and Alzheimer's disease.^{3a} Links between aluminum and several other human diseases, such as amyotrophic lateral sclerosis^{3b} or dialysis encephalopathy,^{3c} have been established.⁴ Experimental evidence suggests that aluminum is epileptogenic.⁵

Aluminum has been shown to interact with DNA.⁶ The interactions of aluminum in model membrane systems show that aluminum binds strongly to the phosphate head groups of the membrane.⁷ The neurotoxicity of Al(III) is also manifested by inhibiting a number of enzymes, such as acetylcholine esterase and Na^+ , K^+ ATPase.⁸ It is plausible that, once bound to ATP,

Al(III) interferes with Mg(II), so that any consequent reactions requiring the Mg(II)-ATP complex participation are inhibited.⁹

In that context, it is of prime importance to specify the interactions of ATP with Al(III) at physiological pH. A few studies have appeared in the recent literature showing that ATP and its Al(III) complex(es) are in slow exchange on the ^{31}P NMR time scale.^{1b,10}

In this paper it is shown that, at pH 7.4, ATP is in slow equilibrium, on the ^{31}P NMR time scale, with complexes of stoichiometries 1:1 ($\text{Al}^{\text{III}}\text{ATP}$; ML) and 1:2 ($\text{Al}^{\text{III}}(\text{ATP})_2$; ML_2), whose respective apparent equilibrium constants of formation were determined. The rate of dissociation of the 1:2 complex was determined by ^{31}P - ^{31}P EXSY 2-D NMR. It is also shown that several forms of the 1:2 complex coexist in moderately fast exchange, with lifetimes in the range 10^{-4} – 10^{-5} s.

Experimental Section

Chemicals and Solutions. ATP stock solutions were prepared by dissolving the crystalline hydrated disodium salt of ATP (Sigma No. A2383, 99% pure by ^{31}P NMR; tetrahydrated; mol. wt 623) in 20% D_2O solution and then adjusted to pH = 6.00 with ultra pure solid sodium hydroxide pellets (Aldrich ultra pure, 99.99%). In some cases the concentration of ATP was checked by UV spectroscopy on the absorbance at 259 nm at pH 7.00. The measured and calculated concentrations always agreed in a 3% range. Aluminum stock solutions in 20% D_2O (typically 0.2 M) were prepared from $\text{AlCl}_3 \cdot x\text{H}_2\text{O}$ (Aldrich gold label, 99.999%) and standardized by complexometric titration using EDTA.¹¹ Aluminum-ATP NMR samples (4 mL) were prepared by mixing, in the following order, the appropriate amount of ATP solution, 20% D_2O solution, and the Al(III) solution using micropipettor syringes. Finally, the pH was adjusted to 7.40 with solid sodium hydroxide pellets. In order to avoid hydrolysis, ATP stock solutions and Al(III)-ATP samples were prepared just prior to NMR experiments and kept in refrigerator. In all cases double distilled water was used.

* Abstract published in *Advance ACS Abstracts*, May 15, 1994.

- (1) (a) *Metal Ions in Biological Systems*; Sigel, H., Ed.; Marcel Dekker: New York, 1988; Vol. 24: Aluminum and its role in biology. (b) Panchalingam, K.; Sachedina, S.; Pettegrew, J. W.; Glonek, T. *Int. J. Biochem.* 1991, 23, 1453–1469. (c) Peri, D. P. In ref 1a, Chapter 7, pp 259–279. (d) Corain, B.; Tapparo, A.; Sheikh-Osman, A. A.; Bombi, G. G.; Zatta, P.; Favaro, M. *Coord. Chem. Rev.* 1992, 112, 19–32. (e) Corain, B.; Nicolini, M.; Zatta, P. *Coord. Chem. Rev.* 1992, 112, 33–45.
- (2) (a) Good, P. F.; Peri, D. P. *Nature* 1993, 362, 418. (b) Landsberg, J. P.; McDonald, B.; Watt, F. *Nature* 1992, 360, 65–68. (c) Candy, J. M.; Oakley, A. E.; Klinowski, J.; Carpenter, T. A.; Perry, R. H.; Atack, J. R.; Perry, E. K.; Blessed, G.; Fairbairn, A.; Edwardson, J. A. *The Lancet* 1986, 354–357.
- (3) (a) Martyn, C. N.; Osmond, C.; Edwardson, J. A.; Barker, D. J. P.; Harris, E. C.; Lacey, R. F. *Lancet* 1989, 1, 59–62. (b) Garruto, R. M.; Fukatsu, R.; Yanagihara, R.; Gajdusek, C.; Hook, G.; Fiori, C. E. *Proc. Natl. Acad. Sci. U.S.A.* 1984, 81, 1875–1879. (c) Alfrey, A. C. *Annu. Rev. Med.* 1978, 29, 93–98.
- (4) Martin, R. B. In *Metal Ions in Biological Systems*; Sigel, H., Ed.; Marcel Dekker: New York, 1988; Vol. 24, pp 1–57.
- (5) Sturman, J. A.; Wisniewski, H. M. In *Metal Neurotoxicity*; Bondy, S. C., Prasad, K. N., Eds.; CRC Press: Boca Raton, FL, 1988; pp 61–85.
- (6) Dyrssen, D.; Haraldsson, C.; Nyberg, E.; Wedborg, M. *J. Inorg. Biochem.* 1987, 29, 67–75.
- (7) Deleers, M.; Servais, J.-P.; Wulfert, E. *Biochim. Biophys. Acta* 1985, 813, 195–200.

(8) Lai, J. C. K.; Guest, J. F.; Leung, T. K. C.; Lim, L.; Davison, A. N. *Biochem. Pharmacol.* 1980, 29, 141–146.

(9) Kiss, T.; Sovago, I.; Martin, R. B. *Inorg. Chem.* 1991, 30, 2130–2132.

(10) (a) Laussac, J.-P.; Commenges, G. *Now. J. Chim.* 1983, 7, 579–585. (b) Karlik, S. J.; Elgavish, G. A.; Eichhorn, G. L. *J. Am. Chem. Soc.* 1983, 105, 602–609. (c) Bock, J. L.; Ash, D. E. *J. Inorg. Biochem.* 1980, 13, 105–110.

(11) *Vogel's, Textbook of Quantitative Chemical Analysis*, 5th ed.; Longman: London, 1989.

All pHs were adjusted to ± 0.05 unit from the reported value and measured with a 3-mm electrode (Ingold Electronics) using a Corning 155 pH meter; pH values in D_2O solutions were corrected for the deuterium isotope effect by adding 0.40 to the meter reading.

Phosphorus spin-lattice relaxation time measurements are extremely sensitive to paramagnetic impurities and need special care.¹² The 20% D_2O solution used to prepare all T_1 samples was passed twice through a column filled with a cation-exchange resin (Amberlite IR-120, sodium form). Paramagnetic ions in ATP were removed by adding and stirring 2 g of the dry resin into the 25-mL ATP stock solution. Typically 0.1 mM of solid $EDTANa_4$ (Aldrich, 98%) was added to the 4-mL aluminum-ATP NMR samples, and removal of oxygen was carried out in the NMR tube by argon bubbling for 15 min. Every sample was then sealed with parafilm.

NMR Measurements. ^{31}P NMR spectra were recorded at five different magnetic fields (1.88, 4.70, 7.05, 11.74, and 14.09 T) on Varian FT-80, Gemini 200, Varian XL-300, Bruker AMX-500, and AMX-600 spectrometers at 32.4, 81.0, 121.4, 202.4, and 242.9 MHz, respectively. D_2O (20%) was used as an internal field lock, and the chemical shifts were referenced to 85% inorganic orthophosphoric acid. The experiments were performed with or/and without proton-decoupling in a 5- or 10-mm (1.88T) probe. In addition, a time constant introducing 0.5–5.0-Hz line broadening was applied as needed to improve signal-to-noise ratios.

1H NMR spectra were recorded locked at 300 and 500 MHz in D_2O solution using a 5-mm tube. ^{13}C measurements were conducted at 75.4 MHz under proton-decoupling conditions in a 10-mm tube. A 20% D_2O solution was used to catch the internal field lock, and all ^{13}C NMR spectra are referenced to internal 1,4-dioxane ($\delta = 67.40$ ppm with respect to TMS). ^{27}Al NMR spectra were obtained at a frequency of 130.3 MHz on a Bruker AMX-500 instrument equipped with a 5-mm broad band probe. All spectra were recorded locked in 20% D_2O solution, and the chemical shifts are referenced to external 0.10 M $AlCl_3$ in D_2O .

^{31}P and ^{13}C spin-lattice relaxation rates ($1/T_1$) were measured using the inversion recovery pulse sequence. In all the cases the recycle time was taken as $\geq 5T_1$. T_1 was obtained from a generalized three-parameter nonlinear regression analysis, in order to account for pulse imperfections.^{13a} ^{31}P and 1H spin-spin relaxation rates ($1/T_2$) were obtained directly from the full width at half-height of the signals ($1/T_2 = \pi\Delta\nu_{1/2}$). The line widths of the ^{31}P NMR signals were corrected for the phosphorus-phosphorus coupling constant using a homemade simulation program.

The ^{31}P - ^{31}P EXSY 2D spectra were obtained at 202.4 MHz with the NOESY pulse sequence.^{13b} The number of scans were 16 for each of the 128 t_1 values, and the mixing time (τ_m) values ranged from 50 to 700 ms. The digital resolution in the F_2 dimension was 7.8 Hz. Two-dimensional 1H NOESY spectra were recorded at 300 MHz using eight different mixing times. To obtain an adequate signal-to-noise ratio, 16 transients were accumulated for each of the 128 FIDs. All experiments, except when stated otherwise, were carried out at (300.0 \pm 0.5) K. The spectrometer variable-temperature unit was calibrated using a copper-constantan thermocouple.

The errors are indicated as one standard deviation (one σ).

The species distribution curves were calculated using a modified version of the SOLGASWATER program.¹⁴

Results

A series of ^{31}P NMR spectra at 121.4 MHz of ATP (structure I) in the presence of various amounts of $Al(III)$ are shown on Figure 1. The three characteristic ^{31}P resonances of ATP (not decoupled from 1H) are observed at -6.0 ppm (doublet; γ -P), -10.2 ppm (doublet of multiplets; α -P), and -20.8 ppm (triplet; β -P). These values are in good agreement with previously reported values for ATP at pH close to 7.4.^{10b} As the concentration of $Al(III)$ increases, two broad resonances appear at approximately -11.4 and -21.6 ppm. The intensities of these resonances increase with the $Al(III)$ concentration. A third broad resonance occurs underneath the α peak at approximately -9.8 ppm. This is more

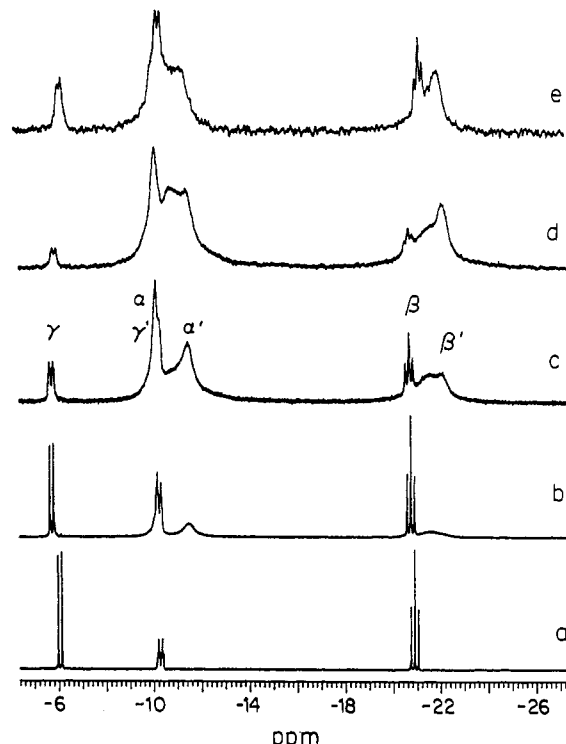
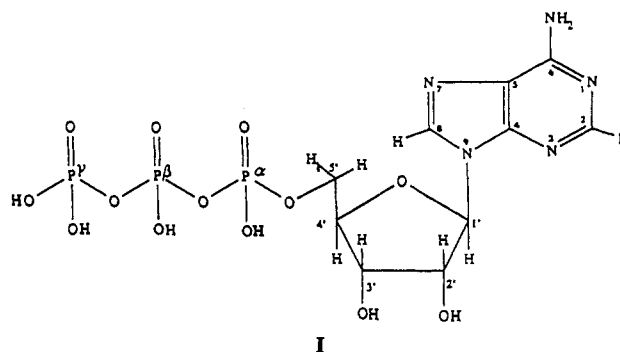


Figure 1. ^{31}P NMR spectra (7.05 T) of ATP aqueous solutions (pH = 7.4) in the presence of $AlCl_3$: (a–d) $[ATP]_T = 100$ mM; (e) $[ATP]_T = 10$ mM; $R = [Al(III)]_T/[ATP]_T = 0$ (a), 0.30 (b), 0.60 (c), 0.90 (d, e). See text for the signals attribution.



apparent either at 242.9 MHz (see Figure 4a) or at higher temperature (see Figure 7). The three broad resonances are attributed (from high to low frequencies) to the γ -, α -, and β -P of an Al^{III} ATP complex. This attribution will be confirmed below (see Figure 7). The three resonances will be referred to as γ' -, α' -, and β' -P, respectively (see Figure 1c). For ratios of total concentrations of $Al(III)$ over total concentration of ATP ($R = [Al(III)]_T/[ATP]_T$) higher than 0.4 a second series of broad resonances can be observed. The spectra for two total concentrations of ATP (100 and 10 mM; same R value) are also given for comparison (Figure 1d,e, respectively).

From the integrations of the ^{31}P NMR spectra, one can easily determine the normalized ratio of complexed ATP ($([L_T] - [L])/[L_T]$), since the integrations of the γ -P and of the β, β' -P signals are respectively proportional to noncomplexed (L) and total (L_T) ATP concentrations. Titration curves of ATP by $Al(III)$ are shown on Figure 2 for three different total ATP concentrations. Qualitatively, one observes two regions in the curves: a steep increase of the complexed ATP concentration at low $Al(III)$ concentrations ($0 < R < 0.4$) and a more pronounced curvature, leading to the full complexation of ATP for large values of $[Al(III)]_T$. This is in good agreement with the observations of Figure 1, showing the appearance of a second type of complex for $R > 0.4$. The slope of the tangent as the origin of the three curves

(12) McCain, D. C.; Markley, J. L. *J. Am. Chem. Soc.* **1980**, *102*, 5559–5565.

(13) (a) Levy, G. C.; Lichter, R. L.; Nelson, G. L. *Carbon-13 Nuclear Magnetic Resonance Spectroscopy*, 2nd ed.; J. Wiley & Sons: New York, 1980; p 226. (b) Ernst, R. R.; Bodenhausen, G.; Wokaun, A. *Principles of Nuclear Magnetic Resonance in One and Two Dimensions*; Oxford Univ. Press: New York, 1987.

(14) Eriksson, G. *Anal. Chim. Acta* **1979**, *112*, 375–385.

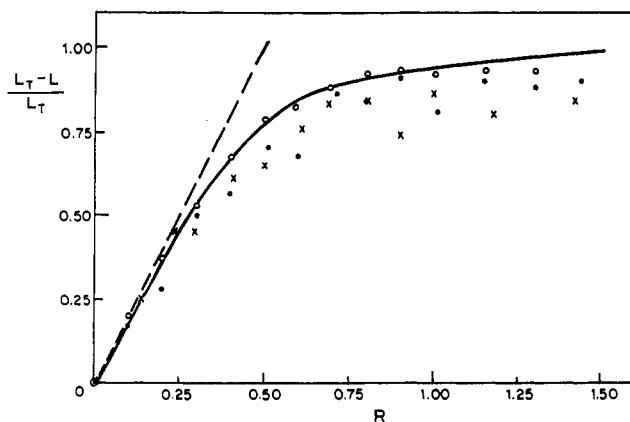


Figure 2. Titration curves of ATP by Al(III) obtained from ^{31}P NMR. The fraction of complexed ATP is expressed as a function of $R = [\text{Al(III)}]_{\text{T}}/[\text{ATP}]_{\text{T}}$. $[\text{ATP}]_{\text{T}} = 100 \text{ mM}$ (O), 40 mM (●), and 10 mM (×).

Table 1. Apparent Equilibrium Constants of Formation of the Complexes ML and ML_2 (Eqs 1 and 2) Calculated from a Nonlinear Regression Analysis on Eq 3 at Different Total ATP Concentrations

$[\text{ATP}]_{\text{T}}$ (mM)	$\log K_1$	$\log K_2$
10	2.5 ± 0.5	2.5 ± 0.4
40	2.6 ± 0.3	1.7 ± 0.2
100	2.0 ± 0.2	2.0 ± 0.2
average	2.4 ± 0.3	2.1 ± 0.4

gives an indication of the stoichiometry of the complex formed at low values of R . It is equal to 2.0, strongly suggesting the formation of an $\text{Al}^{\text{III}}(\text{ATP})_2$ complex. This 1:2 complex coexists with another complex, plausibly of stoichiometry 1:1, which can be detected for R values larger than 0.4 (see Figure 1).

On the basis of the qualitative observations of Figures 1 and 2, a model can be tested. It is based on the simplest assumption of the formation of 1:1 and 1:2 complexes (eqs 1 and 2, where M stands for Al(III) and L for ATP; see the Discussion section for a discussion on the nature of the species involved).



From the mass balance equations and the phenomenological equilibrium constants of formation (K_1 and K_2 , respectively, for eqs 1 and 2), one can express the complex formation function, $\bar{n} = ([\text{L}]_{\text{T}} - [\text{L}])/[\text{M}]_{\text{T}}$, as a function of L , with K_1 and K_2 as adjustable parameters (eq 3).¹⁵

$$\bar{n} = (K_1[\text{L}] + 2K_1K_2[\text{L}]^2)/(1 + K_1[\text{L}] + K_1K_2[\text{L}]^2) \quad (3)$$

A nonlinear regression analysis afforded the results shown in Table 1. Figure 3 shows the plot of \bar{n} as a function of $[L]$. The line was calculated on the basis of the K_1 and K_2 values given in Table 1. As already stated above, for values of $R < 0.4$, only the ML_2 complex is detectable on the ^{31}P NMR spectra. On the basis of the calculated K_1 and K_2 values, for $R = 0.30$, the ratio of the concentrations of ATP in ML_2 over ATP in ML can be calculated to be 5. This corresponds, for a total ATP concentration of 40 mM, to, respectively, 16.7 and 3.3 mM of these two types of ATP. This is in good agreement with the observed NMR spectra. Figure 4 shows ^{31}P NMR spectra at three different fields of observation of a 40 mM ATP solution in the presence of Al(III) ($R = 0.30$). The ML complex is in too low concentration to be detected. The observed ^{31}P line widths of the ML_2 complex (α' -P and β' -P resonances) strongly depend upon the frequency of observation. At low field (1.88 T), the $^2J(^{31}\text{P}_{\alpha'}-^{31}\text{P}_{\beta'})$ coupling

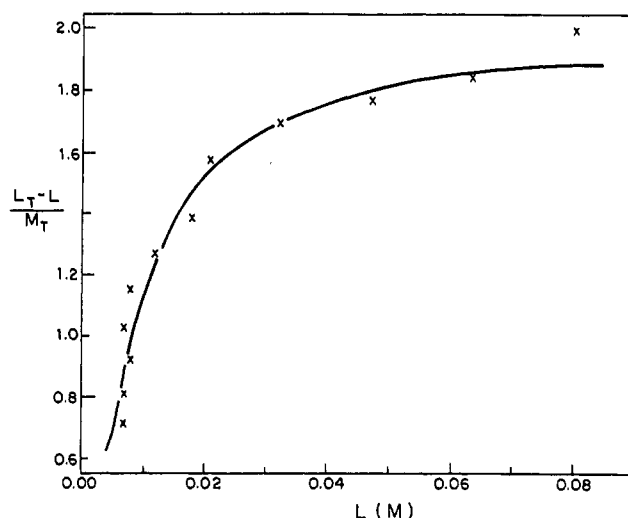


Figure 3. Calculation of the apparent equilibrium constants of formation of the 1:1 and 1:2 complexes. The data points are experimental (obtained from integrations on the ^{31}P NMR spectra), and the curve is calculated from eq 3. $[\text{ATP}]_{\text{T}} = 100 \text{ mM}$.

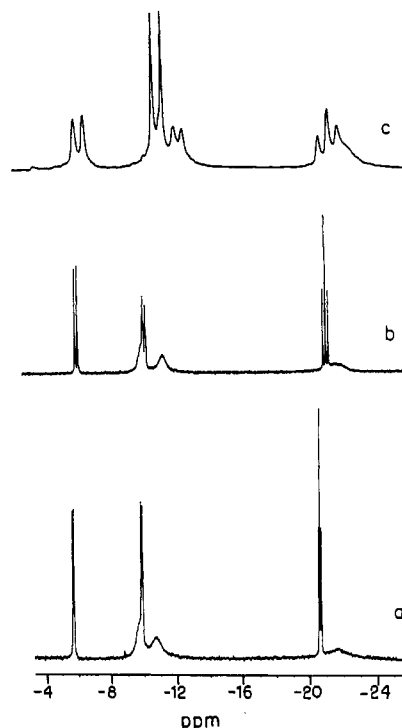


Figure 4. ^{31}P NMR spectra of aqueous ATP solutions (pH = 7.4) in the presence of AlCl_3 at various magnetic fields: (a) 14.09 T; (b) 7.05 T; (c) 1.88 T. $[\text{ATP}]_{\text{T}} = 40 \text{ mM}$ (a, b) and 50 mM (c). $R = [\text{Al(III)}]_{\text{T}}/[\text{ATP}]_{\text{T}} = 0.30$ (a, b) and 0.40 (c).

constant is still observed for α' -P of the complex. All the ^{31}P α' - and β' -P resonances were simulated on the basis of this 2J value, so that line widths could be accurately measured. The transverse relaxation rates derived from these line widths are plotted on Figure 5 as a function of the square of the field of observation. A linear relationship is obtained for the five experimental fields (from 1.88- to 14.09-T instruments). In strong contrast, the longitudinal relaxation rates do not depend upon the field of observation. This eliminates any interpretation based on the chemical shift anisotropy relaxation mechanism. An interpretation based on a ^{31}P - ^{27}Al scalar relaxation of the second kind, for a chemical species in nonextreme narrowing, could also be discarded (see Discussion). The only remaining hypothesis in agreement with the observed T_1 and T_2 behaviors is chemical exchange in the relatively fast limit.¹⁶ This hypothesis can be

(15) Hartley, F. R.; Burgess, C.; Alcock, R. M. *Solution Equilibria*; Ellis Horwood Limited: Chichester, U.K., 1980; Chapter 3, pp 53-72.

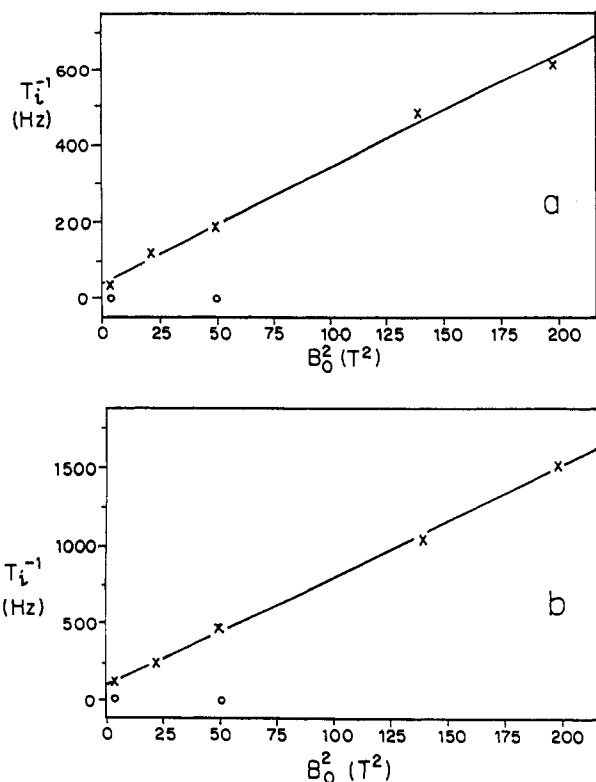


Figure 5. ^{31}P relaxation rates ($(\circ) i = 1$; $(\times) i = 2$) as a function of the square of the field of observation: (a) α' -P signal; (b) β' -P signal. $R = [\text{Al(III)}]_{\text{T}}/[\text{ATP}]_{\text{T}} = 0.30$.

Table 2. ^{31}P NMR-Corrected Line Width of the α' - and β' -P Signals (Figure 1c) of ATP (100 mM; $[\text{Al(III)}] = 25$ mM) at Various Temperatures and at 11.74 T

T (K) (± 0.5 K)	$\nu_{1/2,\text{corr}}$ (Hz)	
	$P_{\alpha'}$	$P_{\beta'}$
275.2	<i>a</i>	178 ^b
281.2	<i>a</i>	234 ^b
291.3	179	345
301.5	136	311
308.6	94	243
315.1	63	183

^a Due to strong overlap with the α - and γ' -P signals, the line widths could not be estimated. ^b Value of the most intense peak (see Figure 6).

further tested by decreasing the temperature. Decreasing the temperature from 315 to 290 K results in an increase of the line width from 183 to 345 Hz (for the β' -P signal). Below that temperature, the observed line width decreases. The data characteristic of this behavior, diagnostic of chemical exchange, are given in Table 2. Figure 6 shows ^{31}P NMR spectra (202.4 MHz) of a 100 mM ATP solution in the presence of various amounts of Al(III) at 275.2 K. Several signals (tentatively four, noted β'_i ($i = 1-4$)) can be observed on each side of the β -P signal (-21 ppm).

In addition to the fast process described above, one can also obtain information on the kinetics of the formation of the ML_2 complex. The exchange is slow on the ^{31}P NMR time scale, since two well distinct peaks are observed for the free and complexed forms. The rate constants were obtained from a series of 2D-EXSY ^{31}P - ^{31}P spectra. The 2D spectrum corresponding to a mixing time of 400 ms is shown on Figure 7 for the region of the α -P and γ -P resonances at 313 K. This temperature was chosen

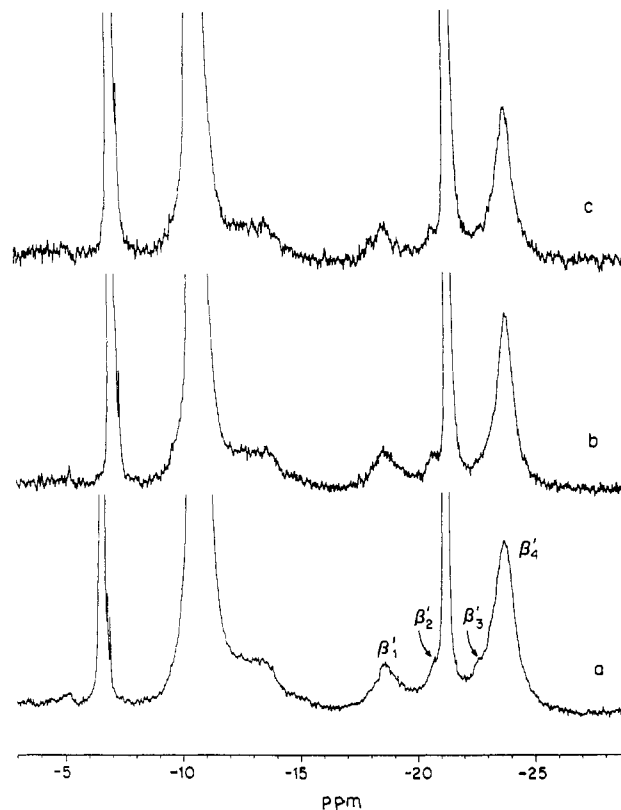


Figure 6. ^{31}P NMR spectra (11.74 T) of aqueous 100 mM ATP solutions at 275.2 K. $R = [\text{Al(III)}]_{\text{T}}/[\text{ATP}]_{\text{T}} = 0.25$ (a), 0.17 (b), and 0.10 (c).

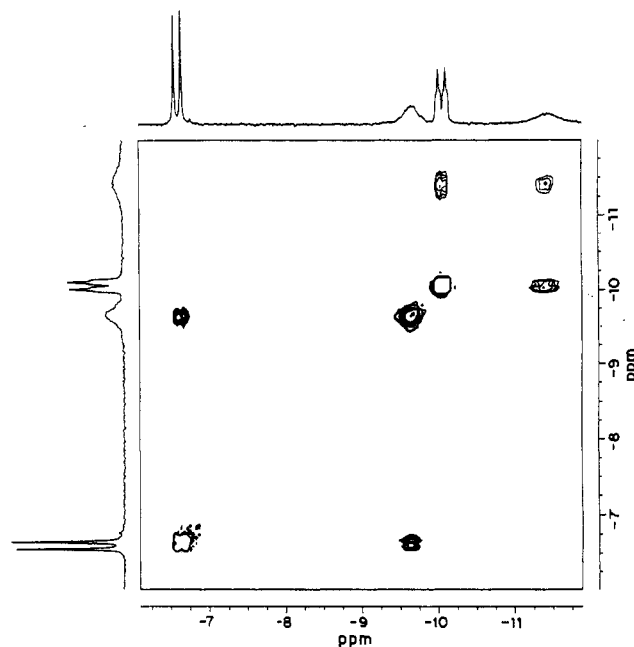


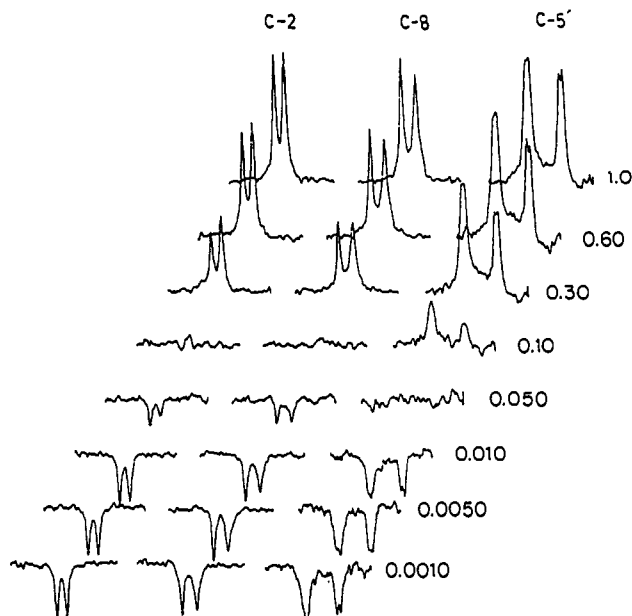
Figure 7. ^{31}P - ^{31}P -EXSY 2D NMR spectrum of an aqueous 100 mM ATP solution in the presence of 25 mM AlCl_3 at 313.0 K. Mixing time = 400 ms.

because of the clear separation between the γ' - and the α -P peaks, and the spectrum confirms the validity of the α' - and γ' -P peaks attributions. Even if this had been assumed in previous works, to the best of our knowledge, this attribution had never been demonstrated. Six different mixing time values, ranging from 50 to 700 ms, were used for the calculation of the rate constant. A nonlinear regression analysis was performed on the equation relating the volume of the cross-peaks to the mixing time,^{17,18} using experimentally determined longitudinal relaxation times. The rate constant characteristic of the exchange was found to be

(16) (a) Delville, A.; Stöver, H. D. H.; Detellier, C. *J. Am. Chem. Soc.* **1987**, *109*, 7293-7301. (b) Detellier, C. In *Modern NMR Techniques and their Applications in Chemistry*; Popov, A. I., Hallenga, K., Eds.; Marcel Dekker: New York, 1991; Chapter 9, pp 521-566. (c) Woessner, D. *E. J. Chem. Phys.* **1961**, *35*, 41-48.

Table 3. Observed ^{13}C Spin–Lattice Relaxation Times and Nuclear Overhauser Effects of the C-2, C-8, and C-5' Resonances of Aqueous 100 mM ATP Solutions ($R = 0$ and 0.40) at 7.05 T

	C-2	C-2c	C-8	C-8c	C-5'	C-5'c
$R = 0$						
$T_{1,\text{obs}}$ (s)	0.42 ± 0.03		0.40 ± 0.03		0.24 ± 0.02	
η_{obs}	1.20 ± 0.05		1.45 ± 0.06		1.73 ± 0.08	
τ_c (ps)	67		86		85	
$R = 0.40$						
$T_{1,\text{obs}}$ (s)	0.33 ± 0.03	0.23 ± 0.01	0.29 ± 0.02	0.20 ± 0.03	0.16 ± 0.01	0.12 ± 0.01
η_{obs}	1.12 ± 0.07	0.96 ± 0.06	1.12 ± 0.07	0.90 ± 0.05	1.44 ± 0.08	1.35 ± 0.10
τ_c (ps)	65	81	82	82	81	94

**Figure 8.** ^{13}C inversion recovery experiment (^1H decoupled) of the free and complexed C-2, C-8, and C-5' ATP resonances at 294 K . The chemical shifts (in ppm) are as follows: C-2, 153.40 and 153.21; C-8, 140.57 and 140.28; C-5', 65.91 and 66.53 (respectively for free and complexed ATP in each case). $[\text{ATP}]_{\text{T}} = 100\text{ mM}$, and $R = [\text{Al(III)}]_{\text{T}}/[\text{ATP}]_{\text{T}} = 0.40$. The delay times (in s) are indicated on the right side of the spectra.

$(3.4 \pm 1.0)\text{ s}^{-1}$, the average value of the rate constants calculated from the $\alpha\text{-P}$ and $\gamma\text{-P}$ cross-peaks (4.1 and 2.7 s^{-1} , respectively). A value of $\approx 2\text{ s}^{-1}$ would be obtained from the approximate equation assuming equality of the T_1 values for the two sites.^{18b} This value is in good agreement with the independently determined rate constant of exchange obtained at 295 K from ^1H 2-D EXSY spectra of the H-2 proton of the adenine base ($0.8 \pm 0.2\text{ s}^{-1}$). An upper limit of the exchange rate of $\text{Sc}^{\text{III}}(\text{ATP})_2$ was estimated¹⁹ to be 12 s^{-1} .

To obtain more information on the microdynamics of the complex, a ^{13}C longitudinal relaxation rate study was undertaken. Figure 8 shows a series of partial ^{13}C spectra, obtained for the inversion-recovery sequence, for the regions of C-2 and C-8 of the adenine base and for C-5' of the sugar moiety. The observed relaxation rates are given in Table 3. Since it is known from the 2D ^{31}P and ^1H EXSY experiments that the rate constant for the exchange between free and complexed ATP is in the order of magnitude of s^{-1} , the ^{13}C T_1 's, in this time scale also, should be affected by the exchange. Under this condition, one can obtain²⁰ the values of T_1 in the absence of exchange, $T_{1,i}$, where $i = f$ or c , respectively, for free and complexed ATP, since the rate constant

is known from the ^{31}P – ^{31}P EXSY experiment described above. The dipolar contribution to the longitudinal relaxation time was obtained from T_1 and the corresponding NOE (Table 3).²¹ The effective correlation times, τ_c , can then be calculated, under the extreme narrowing condition, from the dipolar contribution to the longitudinal relaxation rate.²¹ They are also reported in Table 3. The correlation times determined for free ATP are almost identical at $R = 0$ and $R = 0.40$. This shows the validity of our approach, or, to put it in a different way, there is an excellent agreement between τ_{ex} determined by ^{31}P – ^{31}P EXSY and by ^{13}C T_1 's.

Discussion

The pH of all the solutions was controlled to be 7.4. This value was chosen as a good compromise, since it is in the range of the measured normal tissue values^{1b,22} and enough above the pK_a of $\gamma\text{-P}$ (6.7)^{10a,23} to result in a nearly complete deprotonation of all three phosphate groups. This is confirmed by the value of the $\gamma\text{-P}$ chemical shift (-6 ppm)^{10a} and by the narrowness of the $\gamma\text{-P}$ signal (see Figure 1a): it has been reported^{1b} that the protonation chemical exchange produces a broadening of the $\gamma\text{-P}$ signal, which we do not observe.

In contrast to most mono- and divalent cations causing a high frequency chemical shift variation of the ^{31}P ATP signals upon complexation,²⁴ Al(III), like other trivalent cations,^{10c,19} produces a low-frequency shift. The phosphate ^{31}P chemical shifts depend on the O–P–O bond angles^{25a} and on the phosphate torsional angles.^{25b–d} These effects are coupled and can result in shifts of several ppm. A change from a trans to a gauche conformation produces a low-frequency shift.^{25c} Consequently, the ^{31}P low-frequency shift observed when ATP complexes Al(III) or other trivalent cations could be attributed to the folding of the triphosphate chain to form a tridentate $\text{M}^{\text{III}}\text{ATP}$ complex. Because of these conformational effects, it is not possible to correlate directly the ^{31}P chemical shifts to coordination sites. However, the formation of α,β,γ -tridentate complexes of Al(III) would be in agreement with the ^{17}O NMR results of Shyy *et al.*¹⁹ on the complexes of ATP with Sc(III), La(III), and Lu(III). That Al(III) be coordinated by the triphosphate chain only is supported by the ^1H NMR results: a set of resonances appears at low frequencies from the free ATP ones when Al(III) is present in the solution. The shifts are similar for H-8 and H-2 of the adenine base (0.16 and 0.11 ppm , respectively). These data can be interpreted by some stacking of the adenine bases in the 1:2 complex.

- (17) (a) Jeener, J.; Meier, B. H.; Bachmann, P.; Ernst, R. R. *J. Chem. Phys.* **1979**, *71*, 4546–4553. (b) Reference 13, Chapter 9.
 (18) (a) Brière, K. M.; Dettman, H. D.; Detellier, C. *J. Magn. Reson.* **1991**, *94*, 600–604. (b) Perrin, C. L.; Dwyer, T. *J. Chem. Rev.* **1990**, *90*, 935–967.
 (19) Shyy, Y.-J.; Tsai, T.-C.; Tsai, M.-D. *J. Am. Chem. Soc.* **1985**, *107*, 3478–3484.
 (20) Amat, E.; Cox, B. G.; Rzeszotarska, J.; Schneider, H. *J. Am. Chem. Soc.* **1988**, *110*, 3368–3372.

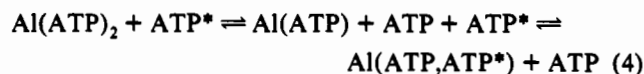
- (21) (a) Harris, R. K. *Nuclear Magnetic Resonance Spectroscopy*; Pitman: London, 1983; Chapter 3. (b) Detellier, C.; Robillard, M. *Can. J. Chem.* **1987**, *65*, 1684–1687.
 (22) Adler, S. In *NMR: Principles and Applications to Biomedical Research*; Pettegrew, J. W., Ed.; Springer: New York, 1989; pp 485–505.
 (23) Labotka, R. J.; Glonek, T.; Myers, T. C. *J. Am. Chem. Soc.* **1976**, *98*, 3699–3703.
 (24) (a) Bock, J. L. *J. Inorg. Biochem.* **1980**, *12*, 119–130. (b) Brown, S. G.; Hawk, R. M.; Komoroski, R. A. *J. Inorg. Biochem.* **1993**, *49*, 1–8.
 (25) (a) Gorenstein, D. G. *J. Am. Chem. Soc.* **1975**, *97*, 898–900. (b) Gorenstein, D. G.; Kar, D. *Biochem. Biophys. Res. Commun.* **1975**, *65*, 1073–1080. (c) Gorenstein, D. G. in *Phosphorous-31 NMR: Principles and Applications*; Gorenstein, D. G., Ed.; Acad. Press: New York, 1984; Chapter 1, pp 19–23. (d) Giessner-Prettre, C.; Pullman, B.; Ribas Prado, F.; Cheng, D. M.; Iuorno, V.; Ts'o, P. O. P. *Biopolymers* **1984**, *23*, 377–388.

The fraction of complexed ATP, as reported in Figure 2, was measured from the integrations of the ^{31}P NMR signals in the regions of $\gamma\text{-P}$ and of $\beta,\beta'\text{-P}$, whose ratio gives the fraction of uncomplexed ATP. The measurement is based on the assumption that the signal at -6.0 ppm can be fully attributed to uncomplexed ATP. Where the integrations of the α' and of the β' signals can be independently done with enough precision, we find the assumption to be valid (the α' - and β' -P signals area are equal to the $\alpha,\gamma\text{-P}$ area from which the $\beta\text{-P}$ area is subtracted).

Only a few studies have reported stability constants for the formation of $\text{Al}^{\text{III}}\text{ATP}$ complexes.^{9,26} Using the constants recently reported by Kiss *et al.*,⁹ it is possible to calculate the species distribution for the solutions used in this work (supplementary material). On the basis of these curves, the ^{31}P "ML₂" peaks ($\delta = -11.4$ and -21.6 ppm, the only signals of complexed ATP observed for $R < 0.4$) should each result from the fast averaging of the signals of two complexes, namely the 1:2 complex, AlL_2 , and its hydroxo derivative, AlL_2OH , while the "ML" peak (observed for $R > 0.4$) corresponds to AlLOH . Using these data,⁹ it can also be seen that the uncomplexed $\text{Al}(\text{III})$ species is the $\text{Al}(\text{OH})_4^-$ anion. This means that the phenomenological equilibrium constants K_1 and K_2 (eqs 1 and 2) are, respectively, $[\text{AlLOH}]/[\text{Al}(\text{OH})_4^-][\text{L}]$ and $\{[\text{AlL}_2] + [\text{AlL}_2\text{OH}]\}/[\text{AlLOH}][\text{L}]$. These constants can be calculated, at the pH of this study, from the formation constants given by Kiss *et al.*⁹ The result, $\log K_1 = 3.7$ and $\log K_2 = 2.8$, is in reasonable agreement with the values of 2.4 and 2.1 (Table 1), considering that our measurements were made without a fixed ionic strength. The full line on Figure 2, relating the fraction of complexed ATP to the ratio $[\text{Al}(\text{III})]_{\text{T}}/[\text{ATP}]_{\text{T}}$ was also calculated from these stability constants data⁹ for $[\text{ATP}]_{\text{T}} = 10$ mM. Again, there is a reasonable agreement between the ^{31}P NMR integration data and the thermodynamic data. The calculated curve predicts an amount of complexed ATP larger than what is experimentally observed. Even at $R = 1.4$, the observed fraction of complexed ATP is only 0.8. This is translated in a value of the phenomenological equilibrium constant K_1 smaller than the value calculated from the literature data.⁹ A possible interpretation could be that some fraction of the $\gamma\text{-P}$ peak that we attribute to "free" ATP ($\delta = -6.0$ ppm) is due to an uncoordinated $\gamma\text{-P}$ belonging to a complexed (α,β -bidentate?) ATP. This is however unlikely since the $\gamma\text{-P}$ phosphate is the most basic one. In their study, performed at low concentrations (mM range), Kiss *et al.*⁹ neglect the presence of polynuclear complexes at pH's above 7. They assume that the only aluminum species present in basic media is $\text{Al}(\text{OH})_4^-$.^{4,9} However, this species, easily characterized by an ^{27}Al NMR chemical shift of $+80$ ppm,²⁷ could not be observed in the solutions of this study at pH 7.4. Other reports²⁸ have considered the presence of polynuclear species, such as $[\text{Al}_{13}\text{O}_4(\text{OH})_{24}]^{7+}$ ("Al₁₃"), in solutions of pH's above 7, even in the presence of ligand. Despite the assumptions of the thermodynamic model, the large errors associated with the NMR integrations measurements, and the nonconstant ionic strength in the NMR study, the fair agreement between the two techniques is quite comforting.

The rate constant characterizing the complexation of $\text{Al}(\text{III})$ by ATP (3.4 s^{-1}) falls in the range of the rate constants for dissociative ligand substitution on octahedral solvates of $\text{Al}(\text{III})$ ($0.1\text{--}5\text{ s}^{-1}$),^{29a} including the exchange of water molecules in the hydration sphere of $\text{Al}(\text{H}_2\text{O})_6^{3+}$.^{29b,c} The mechanism of the ATP

exchange in the $\text{Al}^{\text{III}}(\text{ATP})_2$ complex is dissociative, the rate being governed by the rupture of $\text{Al}(\text{III})$ -phosphate bonds and the 1:1 $\text{Al}^{\text{III}}\text{ATP}$ complex being probably an intermediate in the exchange process (eq 4).



Similarly to previous reports,¹⁰ we observed a broadening of the ^{31}P signals of the complexed species (Figure 4). Three hypotheses will be examined to account for this broadening: (a) There is scalar relaxation of the second kind, due to the coupling of the quadrupolar ^{27}Al nucleus ($I = 5/2$) with ^{31}P . This hypothesis was suggested previously in the literature.¹⁰ (b) There is a chemical shift anisotropy (CSA) contribution to the relaxation, as shown previously in the case of organometallic compounds.³⁰ (c) There is chemical exchange between two or more chemical species in the moderately fast exchange limit.¹⁶ Since the broadening depends on the field of observation (Figure 5), hypothesis a can be rejected, unless the ^{27}Al quadrupolar nucleus relaxes under nonextreme narrowing conditions, with a correlation time in the nanosecond range. We could also reject this possibility by a comparison of the ^{31}P transverse relaxation rates at two different fields and at different temperatures. The transverse relaxation rate depends on the square of the field of observation, as expected if CSA was operative. However this hypothesis b could be ruled out since the longitudinal relaxation rate does not depend upon the field, while a ratio 7/6 would be expected for T_1/T_2 . Both experimental observations on T_1 and T_2 can be rationalized only if the ^{31}P signal of the complexed ATP is in the moderately fast exchange limit. A temperature variation (Table 2) confirms this hypothesis, and at 281 K and below, the exchange becomes slow enough that several lines (tentatively four) can be observed for the β' region (Figure 6). On the basis of the species distribution curves calculated from the data of Kiss *et al.*⁹ for our concentration conditions (but at 300 K), one can speculate on their attribution: β'_1 and β'_4 would be due to the two forms of the 1:2 complex, AlL_2OH and AlL_2 , respectively. The β'_3 peak could be attributed to the 1:1 complex AlLOH , since it appears at the position of the 1:1 complex (see Figure 1). The fourth signal (β'_2) could be due to AlL , which is unlikely on the basis of the species distribution, to some diastereoisomeric forms of the 1:2 complex, as observed in the case of the complex $\text{Co}^{\text{III}}(\text{NH}_3)_3\text{-}(\text{ATP})_2$ ³¹ and postulated for $\text{La}(\text{ATP})_2$, $\text{Lu}(\text{ATP})_2$, and $\text{Sc}(\text{ATP})_2$,¹⁹ or to the presence of a β,γ -bidentate complex, as it is the case for $\text{Mg}(\text{II})$.³² On the basis of the chemical shift difference between the two extreme peaks (β'_1 and β'_4) a very approximate exchange time can be estimated at 300 K:¹⁶ $\tau_{\text{ex}} = 10^{-4}$ s. The rate constant for the hydrolysis of $\text{Al}(\text{H}_2\text{O})_6^{3+}$ has been measured³³ to be $\approx 10^5\text{ s}^{-1}$ in dilute acidified solutions, a value comparable to the estimate of the exchange rate between the species β'_1 and β'_4 . This order of magnitude of the rate constant for the deprotonation of a water molecule coordinated to $\text{Al}(\text{III})$ is in agreement with tentative attribution of β'_1 and β'_4 to the species AlL_2OH and AlL_2 .

One cannot rule out the alternate interpretation that all four signals are due to diastereoisomers of the 1:2 complex,¹⁹ the hydrolyzed form,⁹ AlL_2OH , being, in each case, in fast exchange with AlL_2 . In this interpretation, the 1:2 complex would consist of diastereoisomeric forms of an octahedral $\text{Al}(\text{III})$ coordinated by two α,β,γ -tridentate ATP molecules. The intramolecular interconversion between these isomers would occur with rate

(26) (a) Jackson, G. E.; Voyi, K. V. *Polyhedron* 1987, 6, 2095–2098. (b) Viola, R. E.; Morrison, J. F.; Cleland, W. W. *Biochemistry* 1980, 19, 3131.

(27) Akitt, J. W.; Gessner, W. J. *Chem. Soc., Dalton Trans.* 1984, 147–148.

(28) Sjöberg, S.; Öhman, L.-O. *J. Chem. Soc., Dalton Trans.* 1985, 2665–2669.

(29) (a) Delpuech, J.-J.; Khaddar, M. R.; Peguy, A. A.; Rubini, P. R. *J. Am. Chem. Soc.* 1975, 97, 3373–3379. (b) Fiat, D.; Connick, R. E. *J. Am. Chem. Soc.* 1968, 90, 608–615. (c) Hugi-Cleary, D.; Helm, L.; Merbach, A. E. *Helv. Chim. Acta* 1985, 68, 545–554.

(30) Randall, L. H.; Carty, A. J. *Inorg. Chem.* 1989, 28, 1194–1196.

(31) Cornelius, R. D.; Hart, P. A.; Cleland, W. W. *Inorg. Chem.* 1977, 16, 2799–2805.

(32) Huang, S. L.; Tsai, M.-D. *Biochemistry* 1982, 21, 951–959.

(33) (a) Fong, D. W.; Grunwald, E. J. *Am. Chem. Soc.* 1969, 91, 2413–2422. (b) Holmes, L. P.; Cole, D. L.; Eyring, E. M. *J. Phys. Chem.* 1968, 72, 301–304. (c) Thomas, S.; Reynolds, W. L. *Inorg. Chem.* 1970, 9, 78–81.

constants in the range 10^4 – 10^5 s⁻¹. Shyy *et al.*¹⁹ have postulated a fast process interconverting diastereoisomers to account for their data in the case of Sc^{III}(ATP)₂, even if this is much faster than the similar exchange between the two diastereoisomers of Co^{III}(NH₃)₄ADP, which could be isolated.³⁴ Second-sphere water molecules would be strongly associated with the complex, perhaps forming an H-bond bridge between the two phosphate chains. The rate for the deprotonation of these second sphere water molecules would be much faster than the corresponding rate for the first sphere ones, and an averaging of the NMR signals for AlL₂OH and AlL₂ would then be expected.

(34) Sammons, R. D.; Frey, P. A.; Bruzik, K.; Tsai, M.-D. *J. Am. Chem. Soc.* **1983**, *105*, 5455–5461.

Acknowledgment. The Natural Science and Engineering Research Council of Canada (NSERC) is gratefully acknowledged for financial support. The Wenner-Gren Center Foundation for Scientific Research (Sweden) is acknowledged for a Fellowship to J.B. We thank Dr. Glen Facey (Ottawa U.) for recording the EXSY experiments and Dr. J. R. Brisson (NRC, Ottawa) for recording ³¹P NMR spectra on their Bruker AMX-600 spectrometer. The modifications to the SOLGASWATER program¹⁴ were done by Dr. I. Puigdomenech.

Supplementary Material Available: Six graphs showing the species distribution in solutions of ATP (10, 40, and 100 mM) in the presence of Al(III) at pH = 7.40. These graphs were calculated from the data of Kiss *et al.*⁹ (6 pages). Ordering information is given on any current masthead page.